S. A. Karamian, J. Adam*

ESTIMATION OF THE SPALLATION-RESIDUE ANGULAR MOMENTUM IN p + Ta, Re REACTIONS

*Permanent address: Institute of Nuclear Physics, Řez, Prague, CZ-25068, Czech Republic

1. Introduction

The fragments mass-charge distribution at intermediate energy of protons is of interest during the decade, the interest has been especially increased since a few recent years because of a problem of long-lived radionuclides transmutation. The electronuclear method of the energy production within the scheme of a subcrytical reactor stimulated by an external beam is another practical problem that requires the studies of proton-induced fragmentation of heavy nuclei in detail. Experimental measurements of the product-nuclide yields have been in particular described in Refs. [1-6]. The Monte Carlo codes are also developed to simulate the product yields at thin or thick targets taking into account primary and secondary reactions and different reaction mechanisms. One of the most developed codes – LAHET, Ref. [7] – is used at the present paper as a reference for the comparison of our experimental results with theory predictions. Other codes are also known, see, for instance, Refs. [6,8] and citations within.

The proton-nucleus interaction at intermediate energy, (0.1-1.0) GeV, is described within multi-step model involving the mechanism of intranuclear cascade, INC, pre-equilibrium emission and the decay of excited residue after equilibration. Fission takes place only at third stage, being in competition with nucleon evaporation, because first and second stages are very fast and there is no time for collective deformation to the saddle point. The total probability of fission, mass distribution and other properties depend on Z, A, E^* and I of the fissile nucleus. In prevailing theory, mean $<Z>$, $<A>$ and $<E^*>$ of the residue are calculated within developed INC + percolation models. Then, using those encounters, the fission distributions are simulated in the statistical model of the compound-nucleus decay. The semiempirical approach is also used to reproduce the properties of fission. The angular momentum coordinate is normally not in account, despite it is important for fission. Another simplification is due to the operation with mean values of the fissile-nuclei parameters. In reality, wide distributions in Z, A, and E^* coordinates after fast steps of the reaction and the correlated variation of parameters take place. The Monte Carlo approach allows the simulation of all properties, but more and more complicated codes should be created.

Thus, it would be desirable to get some additional experimental information, in particular, on the angular momentum, I, for the spallation residue. I-value is linked to the impact parameter of the collision and might be useful both for simulation of the spallation and fission stages. For spallation, this would serve as a test useful to verify the residual parameter magnitudes and for fission, to specify the initial parameters of the fissile nucleus.

2. Cross-section measurements

Irradiations of the Ta and Re targets of natural isotopic composition with protons were performed at the internal and external beams of the Dubna synchrocyclotron at energies of 660, 200 and 100 MeV for Ta targets and 660, 450, 300 and 150 MeV for Re targets, Ref. [5]. A geometry of sandwich targets at external beam was applied to get an absolute calibration of the yields. Al foils were exposed together with Ta or Re, and the cross-section of the reactions with Al were used for calibration. Irradiated targets after some "cooling" time have been transferred to gamma spectroscopic measurements either directly without chemical processing or past chemical separation of elemental fractions. The Ge spectrometers are characterized by energy resolution of about 1.8 keV for ^{60}Co lines, and the standard resolution is conserved up to high count rate, like 20000 counts/s, when 20% dead time already arises. The count rate for each sample was optimized by varying the source-detector distance and/or inserting absorbers made of Pb, Cd and Cu. The efficiency of the detector as a function of γ-ray energy was measured at individual experimental conditions by using the standard sources of ^{152}Eu, ^{154}Eu and ^{228}Th.

A number of atoms can be differentially determined for any identified radionuclide as a result of γ-ray spectra analysis. The quantities of spectroscopic parameters significant for the analysis have been taken from Tables of Isotopes and database available in periodics and via net. The absolute yields and cross-sections were finally obtained for many products of the spallation and fission reactions using measured intensities of the characteristic γ-lines of individual isotopes. The calibration of fluence was performed as described above by known cross-sections for some reactions. The typical accuracy better 15% has been reached for the yield measurements including the statistical errors and systematical inaccuracy due to the detector efficiency measurements and inaccuracy of the tabular values. Some additional systematical error

can be inserted also due to the proton fluence calibration by some standard cross-sections. The latter-error magnitude would not be easy to estimate.

The results of measurements taken at irradiation of Re target with 660 MeV protons are given for example in Table 1. The measured yield values are compared with the ones calculated using the LAHET code, see in Ref. [5], general agreement is clear for the spallation products. Yield and cross-section are decreasing when a mass-number of a product nuclide is deviating more and more from the target mass, means with the increase of a number of emitted in reaction nucleons. Such behavior is well described by calculations. One can see in Table 1 that the cumulative yields are typically much higher than the independent yields of the screened isotopes located near the β-stability line.

Table 1. Yields of radionuclides and mean cross-sections measured after activation of the ^{nat}Re target of a $21g/cm^2$ thickness by 660 MeV protons. The measurement accuracy is typically better 15% with exception for some lowest yields. The theoretically predicted yield values are given in the last column.

Nuclide	$T_{1/2}$	E_γ, keV	Type of yield	Mean σ, mbarn	Yield, atoms/proton	Predicted yield
^{185}Os	93.6 d	646.1	Indep.	4.4	$3.0 \cdot 10^{-4}$	$4.0 \cdot 10^{-4}$
^{184g}Re	38 d	903.3	Indep.	38	$2.58 \cdot 10^{-3}$	$\} 3.5 \cdot 10^{-3}$
^{184m}Re	165 d	920.9	Indep.	11	$7.5 \cdot 10^{-4}$	
^{183}Re	70 d	162.5	EC cum.	62	$4.22 \cdot 10^{-3}$	$3.3 \cdot 10^{-3}$
^{182g}Re	2.67 d	1427.3	Indep.	17	$1.16 \cdot 10^{-3}$	$2 \cdot 10^{-3}$ *)
^{178}W	21.7 d	1340.9	EC cum.	36	$2.45 \cdot 10^{-3}$	$3.7 \cdot 10^{-3}$
^{182}Ta	115 d	1231.0	Indep.	2.3	$1.57 \cdot 10^{-4}$	$2.3 \cdot 10^{-4}$
^{181}Hf	42.6 d	482.0	β⁻ cum.	0.14	$0.95 \cdot 10^{-5}$	$2.1 \cdot 10^{-5}$
$^{179m2}Hf$	25.1 d	453.7	Indep.	0.12	$0.82 \cdot 10^{-5}$	$4.2 \cdot 10^{-5}$ *)
$^{178m2}Hf$	31 y	574.2	Indep.	0.13	$0.9 \cdot 10^{-5}$	$7.3 \cdot 10^{-5}$ *)
^{175}Hf	70 d	343.4	EC cum.	59	$4.01 \cdot 10^{-3}$	$4.1 \cdot 10^{-3}$
^{172}Hf	1.87 y	1093.6	EC cum.	55	$3.74 \cdot 10^{-3}$	$3.9 \cdot 10^{-3}$
^{177m}Lu	160.9 d	418.5	Indep.	0.034	$2.3 \cdot 10^{-6}$	$8 \cdot 10^{-6}$ *)
^{174g}Lu	3.31 y	1241.8	Indep.	0.50	$3.4 \cdot 10^{-5}$	$\} 5.2 \cdot 10^{-5}$
^{174m}Lu	142 d	992.0	Indep.	0.59	$4 \cdot 10^{-5}$	
^{173}Lu	1.37 y	272.2	EC cum.	61	$4.15 \cdot 10^{-3}$	$4.15 \cdot 10^{-3}$
^{171}Lu	8.22 d	739.8	EC cum.	46	$3.13 \cdot 10^{-3}$	$4.0 \cdot 10^{-3}$
^{170}Lu	2 d	985.1	EC cum.	42	$2.86 \cdot 10^{-3}$	$3.8 \cdot 10^{-3}$
^{169}Yb	32 d	307.7	EC cum.	57	$3.88 \cdot 10^{-3}$	$3.7 \cdot 10^{-3}$

Nuclide	$T_{1/2}$	E_γ, keV	Type of yield	Mean σ, mbarn	Yield, atoms/proton	Predicted yield
^{166}Yb	2.36 d	1374.1	EC cum.	39	$2.65\cdot10^{-3}$	$3.6\cdot10^{-3}$
^{168}Tm	93.1 d	720.3	Indep.	0.30	$2.0\cdot10^{-5}$	$1.5\cdot10^{-5}$
^{167}Tm	9.24 d	531.5	EC cum.	50	$3.40\cdot10^{-3}$	$3.3\cdot10^{-3}$
^{166}Dy	3.4 d	1379.6	β^- cum.	≤2	$\leq1.4\cdot10^{-4}$	-
^{160}Tb	72.3 d	1271.9	Indep.	0.17	$1.2\cdot10^{-5}$	$4.2\cdot10^{-7}$
^{156}Tb	5.35 d	534.3	Indep.	0.83	$5.6\cdot10^{-5}$	$2\cdot10^{-5}$
^{155}Tb	5.32 d	367.4	EC cum.	13.4	$0.91\cdot10^{-3}$	$1.5\cdot10^{-3}$
^{153}Gd	242 d	103.2	EC cum.	13	$8.8\cdot10^{-4}$	$1.1\cdot10^{-3}$
^{151}Gd	120 d	243.2	EC cum.	12	$8.1\cdot10^{-4}$	$8.5\cdot10^{-4}$
^{149}Gd	9.4 d	298.5	EC cum.	7.4	$5.0\cdot10^{-4}$	$5.5\cdot10^{-4}$
^{146}Gd	48.3 d	633.7	EC cum.	4.5	$3.1\cdot10^{-4}$	$4.8\cdot10^{-4}$
^{156}Eu	15.2 d	2097.7	β^- cum.	0.19	$1.3\cdot10^{-5}$	-
^{149}Eu	93 d	277.0	EC cum.	8.2	$5.6\cdot10^{-4}$	$6\cdot10^{-4}$
^{148}Eu	54.5 d	550.3	Indep.	0.26	$1.8\cdot10^{-5}$	$7\cdot10^{-5}$
^{147}Eu	24.0 d	601.4	EC cum.	4.5	$3.1\cdot10^{-4}$	$6\cdot10^{-4}$
^{145}Eu	5.94 d	893.7	EC cum.	1.9	$1.3\cdot10^{-4}$	$4\cdot10^{-4}$
^{148g}Pm	5.37 d	914.9	Indep.	0.09	$0.6\cdot10^{-5}$	$\left.\begin{array}{c}\\\end{array}\right\}4.2\cdot10^{-7}$
^{148m}Pm	41.3 d	286.6	Indep.	0.05	$3\cdot10^{-6}$	
^{144}Pm	363 d	476.8	Indep.	0.06	$4\cdot10^{-6}$	$2.3\cdot10^{-5}$
^{143}Pm	265 d	742.0	EC cum.	1.6	$1.1\cdot10^{-4}$	$2.8\cdot10^{-4}$
^{139}Ce	137.7 d	165.8	EC cum.	0.87	$5.9\cdot10^{-5}$	-
^{140}Ba	12.8 d	1596.5	β^- cum.	0.006	$0.4\cdot10^{-6}$	-
^{133}Ba	10.5 y	356.0	EC cum.	0.17	$1.1\cdot10^{-5}$	$2.7\cdot10^{-5}$
^{131}Ba	11.8 d	496.3	EC cum.	0.07	$5\cdot10^{-6}$	$1.5\cdot10^{-5}$
^{121m}Te	154 d	212.3	Indep.	0.15	$1.0\cdot10^{-5}$	$0.8\cdot10^{-5}$ *)
^{113}Sn	115 d	391.7	EC cum.	0.11	$7.5\cdot10^{-6}$	$7\cdot10^{-6}$
^{110m}Ag	250 d	884.7	Indep.	0.06	$4\cdot10^{-6}$	$3\cdot10^{-6}$ *)
^{106m}Ag	8.46 d	1045.8	Indep.	0.1	$7\cdot10^{-6}$	$4\cdot10^{-6}$ *)
^{105}Ag	41.3 d	443.4	EC cum.	0.13	$9\cdot10^{-6}$	$6\cdot10^{-6}$
^{103}Ru	39.3 d	497.1	β^- cum.	0.14	$0.95\cdot10^{-5}$	$7\cdot10^{-6}$
^{102}Rh	206 d	475.1	Indep.	0.12	$0.8\cdot10^{-5}$	$0.8\cdot10^{-5}$
^{100}Pd	3.6 d	2376.1	β^+ cum.	0.01	$0.7\cdot10^{-6}$	$3\cdot10^{-6}$
^{95}Nb	35 d	765.8	Indep.	0.21	$1.4\cdot10^{-5}$	$1.1\cdot10^{-5}$
^{91m}Nb	62 d	1204.8	Indep.	0.018	$1.2\cdot10^{-6}$	$1.7\cdot10^{-5}$ *)
^{95}Zr	64 d	756.7	β^- cum.	0.10	$0.7\cdot10^{-5}$	$5\cdot10^{-6}$
^{88}Zr	83.4 d	392.9	EC cum.	0.27	$1.8\cdot10^{-5}$	$2\cdot10^{-5}$
^{88}Y	106.6 d	898.0	Indep.	0.49	$3.3\cdot10^{-5}$	$1.7\cdot10^{-5}$
^{85}Sr	64.8 d	514.0	β^+ cum.	0.87	$5.9\cdot10^{-5}$	$2.8\cdot10^{-5}$
^{84}Rb	32.9 d	881.6	Indep.	0.48	$3.3\cdot10^{-5}$	$1.6\cdot10^{-5}$
^{83}Rb	86.2 d	520.4	β^+ cum.	0.75	$5.1\cdot10^{-5}$	$3.2\cdot10^{-5}$
^{75}Se	119 d	264.6	β^+ cum.	0.55	$3.7\cdot10^{-5}$	$2.6\cdot10^{-5}$

4

Nuclide	$T_{1/2}$	E_γ, keV	Type of yield	Mean σ, mbarn	Yield, atoms/proton	Predicted yield
[72]Se	8.4 d	834.0	β^+ cum.	0.2	$1.3\cdot10^{-5}$	$4\cdot10^{-6}$
[74]As	17.8 d	595.8	Indep.	0.55	$3.7\cdot10^{-5}$	$1.8\cdot10^{-5}$
[65]Zn	244 d	1115.8	β^+ cum.	0.30	$2\cdot10^{-5}$	$1.4\cdot10^{-5}$
[56]Co	78.8 d	1771.4	EC cum.	0.03	$2\cdot10^{-6}$	$3\cdot10^{-6}$
[59]Fe	44.5 d	1099.3	β^- cum.	0.24	$1.6\cdot10^{-5}$	$1.2\cdot10^{-5}$
[54]Mn	312 d	835.3	Indep.	0.20	$1.3\cdot10^{-5}$	$1.4\cdot10^{-5}$
[52]Mn	5.6 d	1434.1	β^+ cum.	0.022	$1.5\cdot10^{-6}$	$3\cdot10^{-6}$
[48]V	16 d	983.5	EC cum.	0.026	$1.8\cdot10^{-6}$	$5\cdot10^{-6}$

*) *A sum of independent yields of both isomeric and ground states is given as predicted.*

The primary spallation products are rather neutron deficient and during "cooling" time the short-lived nuclei after series of EC and β^+ decays are transformed to the most long-lived member of the isobaric chain. This long-lived isotope serves as a trap accumulated the total yield of a definite mass A. Such feature provides rather simple way for the mass distribution measurements applicable at the case of spallation products. This variant is used in present work, the mass-distribution is defined resulting the measurements of the cumulative yields of rather long-lived nuclides. The cumulative yields are reproduced well using the LAHET code simulation. In general, the agreement is within 20%, at some cases higher deviation takes place. But this is typically for lower yield products, and can be explained both by statistical errors of the measurements and by restricted Monte Carlo statistics, while some regular disagreement is also possible. The experimental details and results of calculations are described systematically in Ref. [5]. At present, the data are analyzed and following aims are of interest: to specify the isomer-to-ground state ratios at the spallation reactions, to estimate the spin magnitude for the spallation residues and to discuss the measured values of a fission-to-spallation ratio.

3. Isomer-to-ground state ratios

Results on isomer-to-ground state ratios are obtained both for reactions of Ta and Re spallation, they are reduced in Table 2. The yields of high-spin isomers of [177m]Lu, [178m2]Hf and [179m2]Hf were successfully measured, however, the ground-state yield could not be deduced from the activity measurements because these nuclides are

stable. Finally, the experimentally measured cross-section for the isomer is taken in ratio to the predicted by LAHET code cross-section for the ground state. Determined this way ratio contains the standard error ($\pm 15\%$) of measurements for the isomer and not well-defined systematical error due to the calculation for the ground state. At the case of lower-spin isomers of ^{148m}Pm and ^{174m}Lu, both isomeric and ground states are radioactive and their γ-lines are identified in the measured spectra. Thus, the ratio is completely experimental, however, the inaccuracy of measurements is higher for them because of low spectroscopic yield of the ^{174}Lu γ-lines and low absolute cross-section for the ^{148}Pm production.

One can see in Table 2 that lower σ_m/σ_g values correspond to higher-spin isomers. This is a normal regularity, and it is now confirmed for the spallation reactions with Ta and Re targets. For the ^{177m}Lu, ^{178m2}Hf and ^{179m2}Hf isomers the σ_m/σ_g ratios are significantly increased when Ta is replaced by Re target. At the same time, the ratio remains constant for ^{174}Lu and even is decreased for ^{148}Pm. As we discuss in detail below, the isomer-to-ground state ratio depends mostly on the spin deficit in reaction: the difference ΔI between the spin of isomer and mean angular momentum of the reaction residue.

Table 2. Isomer-to-ground state ratios at 660 MeV.

Isomer	I^{π}	Type of ratio	Ta		Re	
			σ_m/σ_g	$-\Delta A$	σ_m/σ_g	$-\Delta A$
^{179m2}Hf	$25/2^-$	exp/theor	0.038	3	0.19	8
^{178m2}Hf	16^+	exp/theor	0.021	4	0.12	9
^{177m}Lu	$23/2^-$	exp/theor	0.093	5	0.28	10
^{174m}Lu	6^-	exp/exp$^{*)}$	1.2	8	1.2	13
^{148m}Pm	6^-	exp/exp$^{*)}$	0.9	34	0.5	39

*) Standard errors of measurements are of about $\pm 30\%$.

Residual angular momentum should be in correlation with the number of emitted nucleons ($-\Delta A$). Higher ($-\Delta A$) number means larger excitation and higher value of the transfered linear momentum. Respectively, higher angular momentum arises for the

near peripheral collisions. Thus, a significant growth of σ_m/σ_g for ^{177m}Lu, ^{178m2}Hf and ^{179m2}Hf can be understood as a result of increased by a factor of about 2 number of emitted nucleons. When very many, like 40 nucleons are emitted, such events correspond to the hard collision. Then, higher (-ΔA) number means lower impact parameter and lower angular momentum values, and the decrease of σ_m/σ_g for ^{148}Pm can also be explained. ^{174}Lu is in a middle and the ratio remains constant. The saturation of σ_m/σ_g magnitude is expected for spin-excess situation, and this is probably the case of ^{174}Lu.

A correlation of σ_m/σ_g ratio with the residual angular momentum of the reaction was observed in many studies. For instance, in Ref. [9], the production cross-section for ^{178m2}Hf was measured as a function of ^{4}He-ion energy in ^{176}Yb(^{4}He,2n) reaction, and measured σ_m/σ_g ratio was systematized together with other data – as a function of the maximum spin released in the reaction. Regular dependence was established. Later, in Ref. [10] many reactions for population of other isomer in deformed nuclei near A=180 had been studied, and regular dependence of σ_m/σ_g versus spin deficit ΔI had been demonstrated. It was shown in [10] that the type of the reaction makes also influence onto the σ_m/σ_g dependence, in particular, its slope is not the same for the reactions induced by photons or ^{4}He ions. This is clearly in correlation with the width of the spin distribution of the reaction products.

In Fig.1, experimentally determined σ_m/σ_g values for the ^{178m2}Hf isomer production are systematized versus mean spin <I> at different reactions. Data are taken from Refs. [9 and 11]. Regular dependence in Fig.1 supports the idea to estimate mean angular momentum of the spallation residue using the isomer-to-ground state ratios determined now for ^{178m2}Hf, Table 1. Taking into account spin of the isomer 16, one can find mean angular momentum of the residue to be 8.5 and 15 for Ta and Re targets. At the spallation of 4 or 9 nucleons, mean spin <I> = 8.5 or 15 $\hbar$ is carried in the residue.

The estimation of <I> values for Ta-spallation residue is illustrated in Fig.1. For Re, <I> = 15 is deduced from Fig.1 and Fig.2, see below. As we mentioned above, the σ_m/σ_g dependence might be saturated at the range of spin excess, that restricts the application of the systematics type of Fig.1. But we do not reach yet the spin-excess range, when ΔI is negative; although rather high σ_m/σ_g ratio for Re spallation results in

<I> value near the isomer spin. Thus, <I> estimations look trustable. Measured for other high-spin isomers σ_m/σ_g ratios also support the estimations, because higher ratio corresponds to lower spin of the isomer. This is normal regularity, but quantitative estimations of ΔI are difficult at such case because the σ_m/σ_g systematics is not yet available for the ^{177m}Lu and ^{179m2}Hf isomers.

In statistical theory of nuclear reactions, the isomer-population probability must be defined by the spin dependence of level density, that is exponentially decreased with I^2 growth. On this basis, the systematics of Fig.1 should be rearranged using more natural variable: $(\Delta I)^2$. Such dependence is shown in Fig.2, and many points confirm the exponential fall of σ_m/σ_g as a function of $(\Delta I)^2$. But the latter point taken in the ^{179}Hf$(\gamma,n)^{178m2}$Hf reaction, [11], deviates significantly, and clearly demonstrates the importance of a spin distribution width, not only the mean value <I>. After the transition to $(\Delta I)^2$ parameter, Fig.2, the σ_m/σ_g systematics look simply as a straight line in agreement with statistical theory, and it makes more convenience for estimations. However, such modification does not improve the scattering factor due to the different widths of spin distribution in different reactions. The saturation in the range of spin excess also remains without changes. Moreover the application of $(\Delta I)^2$ makes impossible to operate with positive and negative ΔI values. The $(\Delta I)^2$ magnitude is the same, independent on sign, while σ_m/σ_g values are very different.

To summarize, both variants of σ_m/σ_g systematics, versus <I> or $(\Delta I)^2$ parameters, can be used for our estimation of the spallation residue spin and the result would be identical. The width effect also should not produce a significant error in present estimations. The points corresponded to $(^4$He,2n) reaction are included into the systematics with rather wide distribution, from 0 to I_{max} at the case of compound nucleus formation. The spallation-residue spin distribution has comparable or even larger width. So that, mean spin must be estimated correctly when no significant difference in the width parameters takes place.

4. Fission-to-spallation ratio

As is known, angular momentum modifies significantly the fission barrier increasing the fission probability. A quantitative description within the rotating liquid drop model has been formulated as early as a in Ref. [12]. Later, shell corrections

dependent on spin and deformation had been added. Finally, the developed scheme, in particular [13,14], had been created for calculation of fission barriers dependent on Z, A, E^* and I of fissile nucleus. The phenomenological material is also abundant, for instance [15,16]. The heavy-ion induced fission can be described only provided the angular momentum effect is in account.

Above we estimated mean values of the spallation residue angular momentum to be about 10-15 $\hbar$. A wide distribution is expected as well, thus it would be extended from 0 spin to 25-30 $\hbar$. So high spins influence significantly a fission probability, and the fission-to-spallation ratio should be essentially effected. Below the experimental data are analyzed to look for the presence or absence of such effect.

In Figs. 3 and 4 the mass distributions of products are shown as they have been measured after Ta and Re targets irradiation by protons at 660 MeV. One can see two clearly distinguished peaks belonged to the spallation (right) and fission (left) reaction mechanisms. In section 2 there was given a comment about possibility to find the spallation mass-yield by the cumulative yield of most long-lived isobaric nuclide of definite A. The isobaric nuclide chain must have convenient spectroscopic properties, in fact taking place for some mass numbers. For them mass-yields are determined. This is clear from Figs.3,4 that cumulative method works well because the points at spallation peak demonstrate regular A-dependence without noticeable scattering. The independent yields of screened isobars have been also detected in some cases, and they should be added to the cumulative ones being still much lower in magnitude. The cumulative spallation yields are well reproduced by the LAHET code simulations.

Fission mass yields have also been determined by the cumulative products with addition in some case the independent isobar yields. The curves in Fig.3,4 for fission peak are drawn by points, averaging the noticeable scattering of points. Larger scattering than for spallation products is, in part, due to lower yields and correspondingly higher random errors and, in part, due to the incomplete cumulativity of some yields. The line of most probable charge $Z_p(A)$ for fission fragments is located not far from the β-stability line, and a coefficient of cumulativity depends on the individual properties of the isobaric chain. For many mass-numbers, above 90% of the mass-yield is collected by cumulative product, but in some cases the cumulativity is

clearly incomplete. Such points have been selected and excluded from the presentation in Figs.; the remained ones are possibly scattered because of not absolutely identical cumulativity coefficient.

The latter scattering is obviously most important source of the inaccuracy in estimation of the fission-to-spallation ratio. The spallation and fission peaks have been integrated over corresponding mass ranges and total spallation (σ_s) and fission (σ_f) product cross-sections have been deduced. The curves shown in Figs. are used for interpolations and extrapolations, and the inaccuracy is partially reduced by such smoothing procedure. The decomposition of two processes near A=120 makes no difficulties. The Gaussian fit has not been applied because the spallation peak has definitely another shape, and fission symmetric maximum also can be distorted by other processes. The ternary and multifragmentation yields may be superimposed with the binary fission yield at the mass range of A≤80. The role of multifragmentation was stressed in Ref. [4]. But yet, the probability of binary fission dominates strongly over that of more complicated processes, like ternary fission or miltifragmentation.

A sum of individual mass cross-sections for fission peak has been calculated to determine the double total cross-section of fission: $2\sigma_f$. A factor of 2 is just because two fragments are produced at one fission event. Thus, we assume here that the contribution of multiple processes is negligible, and the fission peak corresponds exclusively to binary fission. An indirect confirmation of that can be found in the fission peak width. For Ta, mass-distribution looks a little wider than for Re target. Such variation could be expected because of Z^2/A parameter of the fissile nucleus changing, and it appeared in the experiment.

The fission-to-spallation ratios, $2\sigma_f/\sigma_s$, are shown in Fig.5 for Ta and Re as a function of the proton beam energy and as a function of Z^2/A at 660 MeV for Ta and Re and at 800 MeV for Au and Pb targets. Two latter points are taken from Refs. [1 and 8], they are in correlation with our results demonstrating the regular increase of the fission probability for heavier targets. As is shown in Fig.5, the accuracy of experimental results is not very high both in present measurement and in Refs. [1,8]. The systematical errors due to some assumptions chosen at the data processing are of importance. Nevertheless some regularities are manifested.

In Fig.5a the experimental points and corresponding guide line for Re target can be compared with the results of simulation. The Monte Carlo code underestimates the fission probability at 660 MeV and predicts drastically decreased probability at lower proton energy. The discrepancy is rather high below 500 MeV. The disagreement with the LAHET code simulation was also notified in Ref. [1] for fission of Au target by 800 MeV protons. Some definite reason has to be responsible for the discrepancy. There is the possibility of the parameter variation within the code, but it reproduces well the cross-sections of spallation, means, the parameters are satisfactory. Exists another possibility to use semiempirical description of fission process, while spallation is still simulated by standard code. This way may be applied if no possibilities for the corrections are found. But in fact, the theoretical model of fission allows many possible modifications. We may propose the consequent account of the angular momentum effect. As was estimated in section 3, mean angular momentum of the spallation residue is not negligible, wide distribution is also expected. The reduction of fission barrier due to rotation of fissile nucleus leads to increase of the fission probability and decrease of the slope of the energy dependence. Just these changes are necessary to improve the agreement between theory and experiment in Fig.5a. It may mean that LAHET code works well as far as the assumptions are correct. Underestimation of the residual angular momentum leads to significant discrepancy in the fission probability simulation.

5. Summary

Measured earlier cross-sections for the isotope and isomer production in irradiation of Ta and Re targets by protons at intermediate energies are analyzed. The isomer-to-ground state ratios for high-spin isomers are defined and used for estimation of a mean spin of the spallation residue. Significant angular momentum value may influence the probability of fission. The fission-to-spallation ratios are evaluated from analysis of experimental data and this ratio dependence on proton energy confirms the angular momentum effect. Other properties are also discussed.
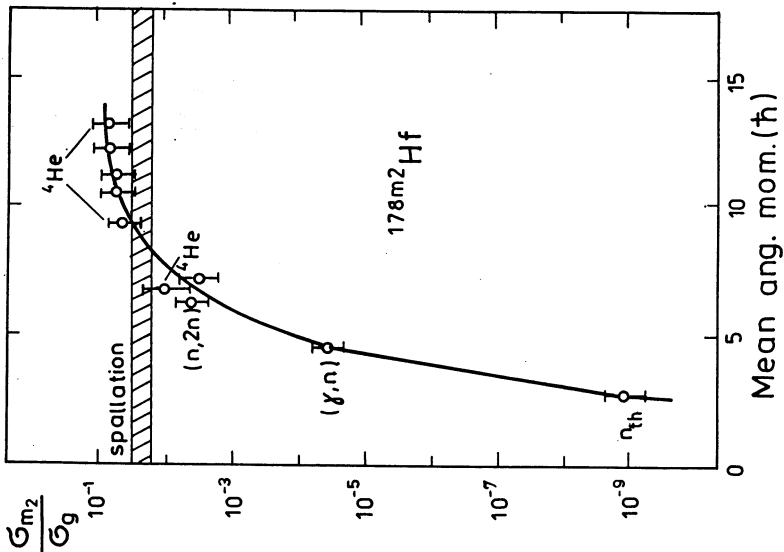
Fig.2. The same, as in Fig.1, but plotted versus $(\Delta I)^2$ parameter, straight line follows the points.

Fig.1. Measured isomer-to-ground state ratios versus residual mean spin values for ^{178m2}Hf production in reactions induced by different projectiles. Points (from Ref. [9]) are connected by a guide line.
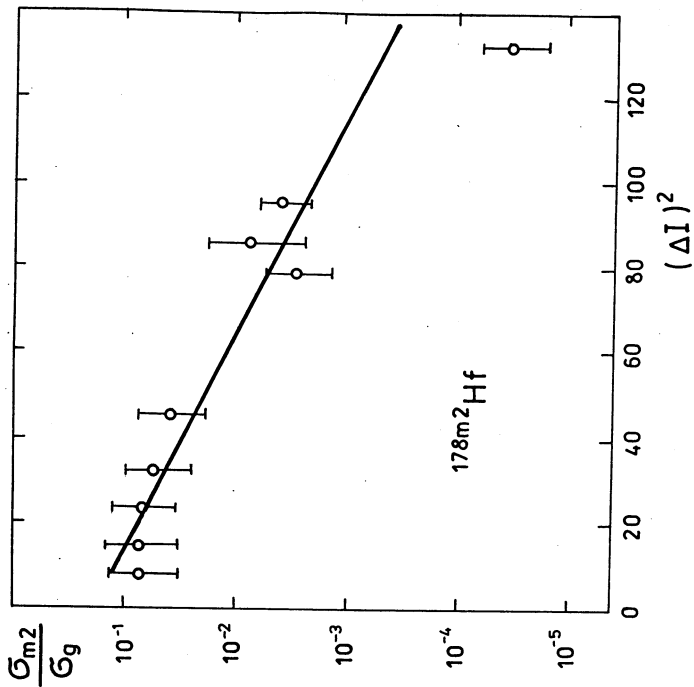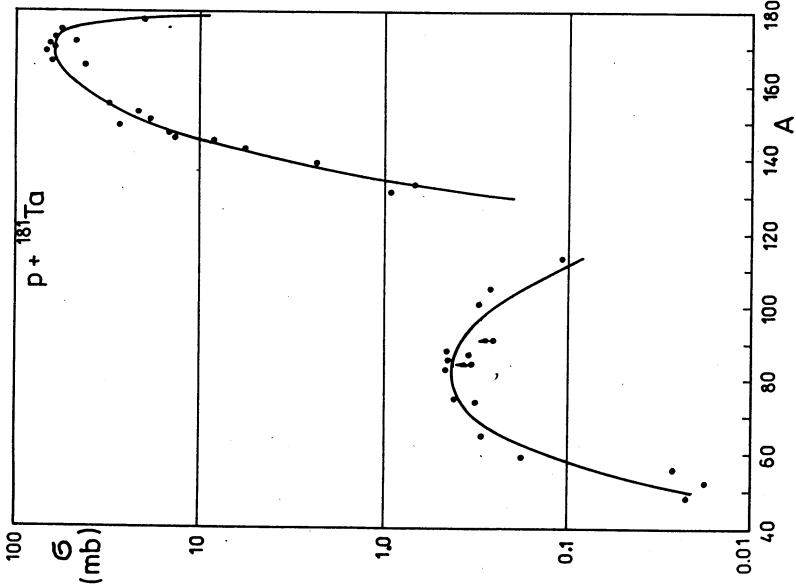
Fig.4. The same, as in Fig.3, but for Re target.

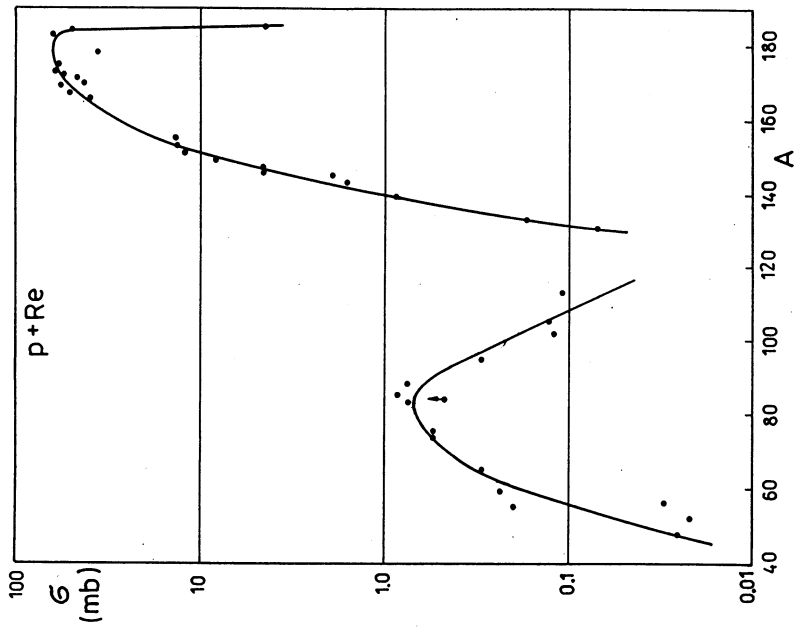Fig.3. Mass distribution of products in p+Ta reaction at 660 MeV. Points correspond to measured values, curve is a guide line.
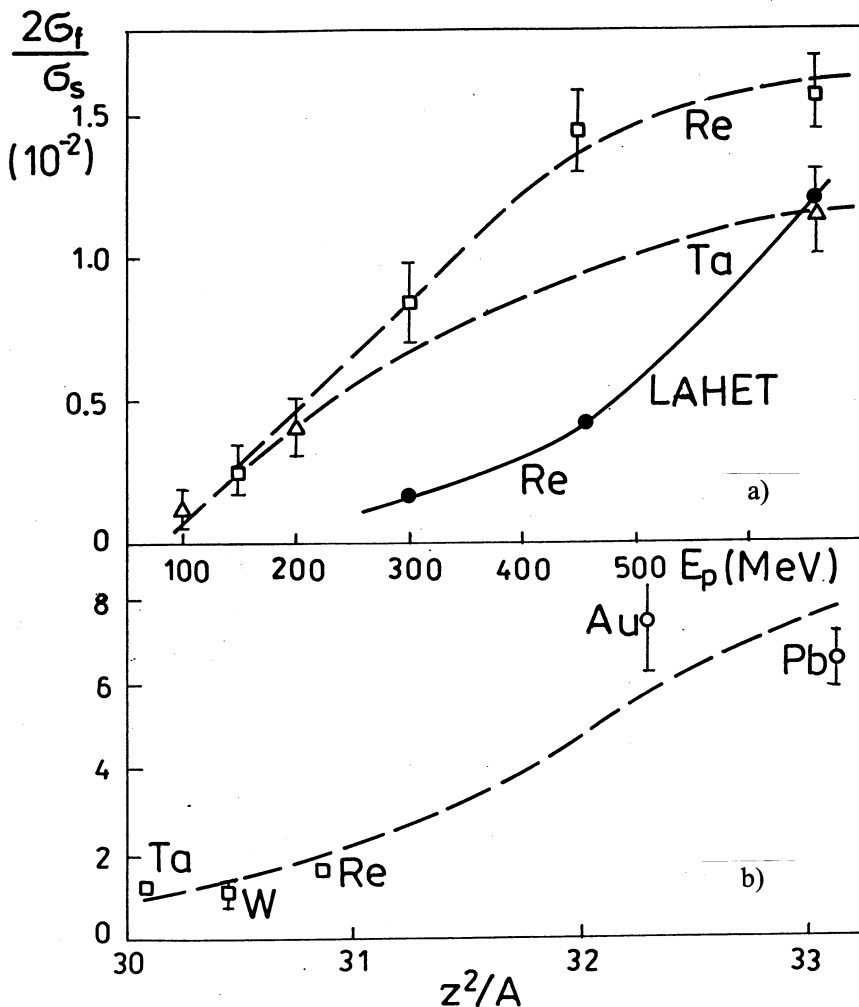
Fig. 5. Fission-to-spallation ratio, 2 σ_f/σ_s, plotted
   a) versus proton beam energy for Ta and Re targets, and
   b) versus Z^2/A of a compound nucleus at 660 MeV for Ta, Re and at 800 MeV for Au, Pb.
Points correspond to measured values for Ta and Re in present work, and for Au and Pb in Refs. [1,8]. Curves are guide lines. The results of LAHET code simulation for Re target, Ref. [5] are also given in part a).

References

1. J. Benlliure, P. Armbruster, M. Bernas et al., Nucl. Phys., A683 (2001) 513.
2. J. Benlliure, P. Armbruster, M. Bernas et al., Nucl. Phys., A700 (2002) 469.
3. V.E. Alexandryan, J. Adam, A.R. Balabekyan et al., Yad. Fyz., 63 (2000) 204.
4. Yu.A. Chestnov and B.Yu. Sokolovsky, Yad. Fyz., 64 (2001) 1541.
5. S.A. Karamian, J. Adam, D.V. Filossofov et al., Preprint JINR E6-2001-249; To appear in Nucl. Instr. Meth. A.
6. Yu.E. Titarenko, O.V. Shvedov, M.M. Igumnov et al., Nucl. Instr. Meth., A414 (1998) 73.
7. R.E. Prael and H. Lichtenstein, LANL Report LA-UR-89-3014, 1989, Los-Alamos.
8. J. Cougnon, C. Volant and S. Vuillier, Nucl. Phys., A620 (1997) 475.
9. Yu.Ts. Oganessian, S.A. Karamian, Yu.P. Gangrski, et al., J. Phys. G18 (1992) 393.
10. S.A.Karamian, J. de Boer, Yu.Ts. Oganessian, et al., Z. Phys., A356 (1996) 23.
11. S.A. Karamian and J.J. Carroll, Las. Phys., 12 (2002) 310.
12. S. Cohen, F. Plasil and W.J. Swiatecki, Ann. Phys. 82 (1974) 557.
13. N. Sierk, Phys. Rev., C33 (1986) 2039.
14. A.V. Ignatiuk, G.N. Smirenkin and A.S. Tishin, Yad. Fiz. 21 (1975) 485.
15. M. Blann, D. Akers, T.A. Komoto, et al., Phys. Rev., C26 (1982) 1471.
16. M.C. Duijvestijn, A.J. Koning and F.J. Hambsch, Phys. Rev. C64 (2001) 014607.

Карамян С. А., Адам И. E6-2002-206
Оценка углового момента для ядра-остатка
реакции скалывания p + Ta, Re

Методом измерения гамма-активности определены выходы и сечения образования радиоактивных изотопов при облучении мишеней из Ta и Re протонами с энергией от 100 до 660 МэВ. Массовое распределение продуктов реакций содержит два широких максимума, соответствующих скалыванию и делению. Среди наблюдаемых нуклидов обнаружены также высокоспиновые изомеры Hf и Lu. На основе измеренного изомерного отношения σ_m/σ_g и с использованием известной систематики σ_m/σ_g в зависимости от спина оценен средний угловой момент I для ядра-остатка реакции скалывания. Ненулевое значение спина I увеличивает вероятность деления ядра. Измеренное отношение сечений деления и скалывания действительно оказалось выше, чем было предсказано по коду Монте-Карло без учета углового момента.

Работа выполнена в Лаборатории ядерных реакций им. Г. Н. Флерова ОИЯИ.

Karamian S. A., Adam J. E6-2002-206
Estimation of the Spallation-Residue Angular Momentum
in p + Ta, Re Reactions

Yields and cross-sections for the radioactive isotope production have been determined via gamma-activity measurements after irradiation of the Ta and Re targets by protons with energies from 100 to 660 MeV. Mass distribution of the reaction products contains two wide peaks corresponding to the spallation and fission product nuclei, respectively. High-spin Hf and Lu isomers are among the detected nuclides. The spallation-residue angular momentum I has been estimated basing on the determined isomer-to-ground state ratio σ_m/σ_g and using known systematics of σ_m/σ_g versus I. Nonzero value of spin I should increase a probability of fission. Measured fission-to-spallation ratio is indeed higher than that predicted by the Monte Carlo code simulation without angular momenta in account.

The investigation has been performed at the Flerov Laboratory of Nuclear Reactions, JINR.

Макет *Т. Е. Попеко*